arXiv:1906.00794v2 [cs.LG] 5 Sep 2019

Blow: a single-scale hyperconditioned flow for non-parallel raw-audio voice conversion

Joan Serrà
Telefónica Research
joan.serra@telefonica.com

Santiago Pascual
Universitat Politècnica de Catalunya
santi.pascual@upc.edu

Carlos Segura
Telefónica Research
carlos.seguraperales@telefonica.com

Abstract

End-to-end models for raw audio generation are a challenge, specially if they have to work with non-parallel data, which is a desirable setup in many situations. Voice conversion, in which a model has to impersonate a speaker in a recording, is one of those situations. In this paper, we propose Blow, a single-scale normalizing flow using hypernetwork conditioning to perform many-to-many voice conversion between raw audio. Blow is trained end-to-end, with non-parallel data, on a frame-by-frame basis using a single speaker identifier. We show that Blow compares favorably to existing flow-based architectures and other competitive baselines, obtaining equal or better performance in both objective and subjective evaluations. We further assess the impact of its main components with an ablation study, and quantify a number of properties such as the necessary amount of training data or the preference for source or target speakers.

1 Introduction

End-to-end generation of raw audio waveforms remains a challenge for current neural systems. Dealing with raw audio is more demanding than dealing with intermediate representations, as it requires a higher model capacity and a usually larger receptive field. In fact, producing high-level waveform structure was long thought to be intractable, even at a sampling rate of 16 kHz, and is only starting to be explored with the help of autoregressive models [1–3], generative adversarial networks [4, 5] and, more recently, normalizing flows [6, 7]. Nonetheless, generation without long-term context information still leads to sub-optimal results, as existing architectures struggle to capture such information, even if they employ a theoretically sufficiently large receptive field (cf. [8]).

Voice conversion is the task of replacing a source speaker identity by a targeted different one while preserving spoken content [9, 10]. It has multiple applications, the main ones being in the medical, entertainment, and education domains (see [9, 10] and references therein). Voice conversion systems are usually one-to-one or many-to-one, in the sense that they are only able to convert from a single or, at most, a handful of source speakers to a unique target one. While this may be sufficient for some cases, it limits their applicability and, at the same time, it prevents them from learning from multiple targets. In addition, voice conversion systems are usually trained with parallel data, in a strictly supervised fashion. To do so, one needs input/output pairs of recordings with the corresponding source/target speakers pronouncing the same underlying content with a relatively accurate temporal alignment. Collecting such data is non-scalable and, in the best of cases, problematic. Thus, researchers are shifting towards the use of non-parallel data [11–15]. However, non-parallel voice conversion is still an open issue, with results that are far from those using parallel data [10].

In this work, we explore the use of normalizing flows for non-parallel, many-to-many, raw-audio voice conversion. We propose Blow, a normalizing flow architecture that learns to convert voice recordings end-to-end with minimal supervision. It only employs individual audio frames, together with an

33rd Conference on Neural Information Processing Systems (NeurIPS 2019), Vancouver, Canada.

identifier or label that signals the speaker identity in such frames. Blow inherits some structure from Glow [16], but introduces several improvements that, besides yielding better likelihoods, prove crucial for effective voice conversion. Improvements include the use of a single-scale structure, many blocks with few flows in each, a forward-backward conversion mechanism, a conditioning module based on hypernetworks [17], shared speaker embeddings, and a number of data augmentation strategies for raw audio. We quantify the effectiveness of Blow both objectively and subjectively, obtaining comparable or even better performance than a number of baselines. We also perform an ablation study to quantify the relative importance of every new component, and assess further aspects such as the preference for source/target speakers or the relation between objective scores and the amount of training audio. We use public data and make our code available at `https://github.com/joansj/blow`. A number of voice conversion examples are provided in `https://blowconversions.github.io`.

2 Related work

To the best of our knowledge, there are no published works utilizing normalizing flows for voice conversion, and only three using normalizing flows for audio in general. Prenger et al. [6] and Kim et al. [7] concurrently propose using normalizing flows as a decoder from mel spectrograms to raw audio. Their models are based on Glow, but with a WaveNet [1] structure in the affine coupling network. Yamaguchi et al. [18] employ normalizing flows for audio anomaly detection and cross-domain image translation. They propose the use of class-dependant statistics to adaptively normalize flow activations, as done with AdaBN for regular networks [19].

2.1 Normalizing flows

Based on Barlow's principle of redundancy reduction [20], Redlich [21] and Deco and Brauer [22] already used invertible volume-preserving neural architectures. In more recent times, Dinh et al. [23] proposed performing factorial learning via maximum likelihood for image generation, still with volume-preserving transformations. Rezende and Mohamed [24] and Dinh et al. [25] introduced the usage of non-volume-preserving transformations, the formers adopting the terminology of normalizing flows and the use of affine and radial transformations [26]. Kingma and Dhariwal [16] proposed an effective architecture for image generation and manipulation that leverages 1×1 invertible convolutions. Despite having gained little attention compared to generative adversarial networks, autoregressive models, or variational autoencoders, flow-based models feature a number of merits that make them specially attractive [16], including exact inference and likelihood evaluation, efficient synthesis, a useful latent space, and some potential for gradient memory savings.

2.2 Non-parallel voice conversion

Non-parallel voice conversion has a long tradition of approaches using classical machine learning techniques [27–30]. However, today, neural networks dominate the field. Some approaches make use of automatic speech recognition or text representations to disentangle content from acoustics [31, 32]. This easily removes the characteristics of the source speaker, but further challenges the generator, which needs additional context to properly define the target voice. Many approaches employ a vocoder for obtaining an intermediate representation and as a generation module. Those typically convert between intermediate representations using variational autoencoders [11, 12], generative adversarial networks [13, 14], or both [15]. Finally, there are a few works employing a fully neural architecture on raw audio [33]. In that case, parts of the architecture may be pre-trained or not learned end-to-end. Besides voice conversion, there are some works dealing with non-parallel music or audio conversion: Engel et al. [34] propose a WaveNet autoencoder for note synthesis and instrument timbre transformations; Mor et al. [35] incorporate a domain-confusion loss for general musical translation and Nachmani and Wolf [36] incorporate an identity-agnostic loss for singing voice conversion; Haque et al. [37] use a sequence-to-sequence model for audio style transfer.

3 Flow-based generative models

Flow-based generative models learn a bijective mapping from input samples $\mathbf{x} \in \mathcal{X}$ to latent representations $\mathbf{z} \in \mathcal{Z}$ such that $\mathbf{z} = f(\mathbf{x})$ and $\mathbf{x} = f^{-1}(\mathbf{z})$. This mapping f, commonly called a normalizing flow [24], is a function parameterized by a neural network, and is composed by a

sequence of k invertible transformations $f = f_1 \circ \cdots \circ f_k$. Thus, the relationship between $\mathbf{x}$ and $\mathbf{z}$, which are of the same dimensionality, can be expressed [16] as

$$\mathbf{x} \triangleq \mathbf{h}_0 \overset{f_1}{\longleftrightarrow} \mathbf{h}_1 \overset{f_2}{\longleftrightarrow} \mathbf{h}_2 \cdots \overset{f_k}{\longleftrightarrow} \mathbf{h}_k \triangleq \mathbf{z}.$$

For a generative approach, we want to model the probability density $p(\mathcal{X})$ in order to be able to generate realistic samples. This is usually intractable in a direct way, but we can now use f to model the exact log-likelihood

$$L(\mathcal{X}) = \frac{1}{|\mathcal{X}|} \sum_{i=1}^{|\mathcal{X}|} \log\left(p\left(\mathbf{x}_i\right)\right). \tag{1}$$

For a single sample $\mathbf{x}$, and using a change of variables, the inverse function theorem, compositionality, and logarithm properties (Appendix A), we can write

$$\log\left(p\left(\mathbf{x}\right)\right) = \log\left(p\left(\mathbf{z}\right)\right) + \sum_{i=1}^{k} \log\left|\det\left(\frac{\partial f_i(\mathbf{h}_{i-1})}{\partial \mathbf{h}_{i-1}}\right)\right|,$$

where $\partial f_i(\mathbf{h}_{i-1})/\partial \mathbf{h}_{i-1}$ is the Jacobian matrix of f_i at $\mathbf{h}_{i-1}$ and the log-determinants measure the change in log-density made by f_i. In practice, one chooses transformations f_i with triangular Jacobian matrices to achieve a fast calculation of the determinant and ensure invertibility, albeit these may not be as expressive as more elaborate ones (see for instance [38–40]). Similarly, one chooses an isotropic unit Gaussian for $p(\mathbf{z})$ in order to allow fast sampling and straightforward operations.

A number of structures and parameterizations of f and f_i have been proposed for image generation, the most popular ones being RealNVP [25] and Glow [16]. More recently, other works have proposed improvements for better density estimation and image generation in multiple contexts [38–43]. RealNVP uses a block structure with batch normalization, masked convolutions, and affine coupling layers. It combines those with 2×2 squeezing operations and alternating checkerboard and channel-wise masks. Glow goes one step further and, besides replacing batch normalization by activation normalization (ActNorm), introduces a channel-wise mixing through invertible 1×1 convolutions. Its architecture is composed of 3 to 6 blocks, formed by a 2×2 squeezing operation and 32 to 64 steps of flow, which comprise a sequence of ActNorm, 1×1 invertible convolution, and affine coupling. For the affine coupling, three convolutional layers with rectified linear units (ReLUs) are used. Both Glow and RealNVP feature a multi-scale structure that factors out components of $\mathbf{z}$ at different resolutions, with the intention of defining intermediary levels of representation at different granularities. This is also the strategy followed by other image generation flows and the two existing audio generation ones [6, 7].

4 Blow

Blow inherits some structure from Glow, but incorporates several modifications that we show are key for effective voice conversion. The main ones are the use of (1) a single-scale structure, (2) more blocks with less flows in each, (3) a forward-backward conversion mechanism, (4) a hyperconditioning module, (5) shared speaker embeddings, and (6) a number of data augmentation strategies for raw audio. We now provide an overview of the general structure (Fig. 1).

We use one-dimensional 2× squeeze operations with an alternate pattern [25] and a series of steps of flow (Fig. 1, left). A step of flow is composed of a linear invertible layer as channel mixer (similar to a 1×1 invertible convolution in the two-dimensional case), ActNorm, and a coupling network with affine coupling (Fig. 1, center). Coupling networks are formed by one-dimensional convolutions and hyperconvolutions with ReLU activations (Fig. 1, right). The last convolution and the hyperconvolution of the coupling network have a kernel width of 3, while the intermediate convolution has a kernel width of 1 (we use 512×512 channels). The same speaker embedding feeds all coupling networks, and is independently adapted for each hyperconvolution. Following common practice, we compare the output $\mathbf{z}$ against a unit isotropic Gaussian and optimize the log-likelihood L (Eq. 1) normalized by the dimensionality of $\mathbf{z}$.

4.1 Single-scale structure

Besides the aforementioned ability to deal with intermediary levels of representation, a multi-scale structure is thought to encourage the gradient flow and, therefore, facilitate the training of very deep

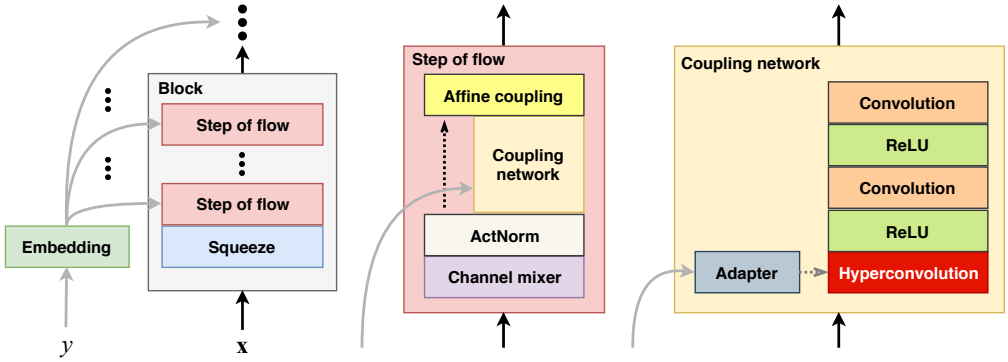


Figure 1: Blow schema featuring its block structure (left), steps of flow (center), and coupling network with hyperconvolution module (right).

models [44] like normalizing flows. Here, in preliminary analysis, we observed that speaker identity traits were almost present only at the coarser level of representation. Moreover, we found that, by removing the multi-scale structure and carrying the same input dimensionality across blocks, not only gradients were flowing without issue, but better log-likelihoods were also obtained (see below).

We believe that the fact that gradients still flow without factoring out block activations is because the log-determinant term in the loss function is still factored out at every flow step (Appendix A). Therefore, some gradient is still shuttled back to the corresponding layer and below. The fact that we obtain better log-likelihoods with a single-scale structure was somehow expected, as block activations now undergo further processing in subsequent blocks. However, to our understanding, this aspect seems to be missed in the likelihood-based evaluation of current image generation flows.

4.2 Many blocks

Flow-based image generation models deal with images between 32×32 and 256×256 pixels. For raw audio, a one-dimensional input of 256 samples at 16 kHz corresponds to 16 ms, which is insufficient to capture any interesting speech construct. Phoneme duration can be between 50 and 180 ms [45], and we need a little more length to model some phoneme transition. Therefore, we need to increase the input and the receptive field of the model. To do so, flow-based audio generation models [6, 7] opt for more aggressive squeezing factors, together with a WaveNet-style coupling network with dilation up to 2^8. In Blow, in contrast, we opt for using many blocks with relatively few flow steps each. In particular, we use 8 blocks with 12 flows each (an 8×12 structure). Since every block has a $2\times$ squeeze operation, this implies a total squeezing of 2^8 samples.

Considering two convolutions of kernel width 3, an 8×12 structure yields a receptive field of roughly 12500 samples that, at 16 kHz, corresponds to 781 ms. However, to allow for larger batch sizes, we use an input frame size of 4096 samples (256 ms at 16 kHz). This is sufficient to accommodate, at least, one phoneme and one phoneme transition if we cut in the middle of words, and is comparable to the receptive field of other successful models like WaveNet. Blow operates on a frame-by-frame basis without context; we admit that this could be insufficient to model long-range speaker-dependent prosody, but nonetheless believe it is enough to model core speaker identity traits.

4.3 Forward-backward conversion

The default strategy to perform image manipulation [16] or class-conditioning [41, 42] in Glow-based models is to work in the $\mathbf{z}$ space. This has a number of interesting properties, including the possibility to perform progressive changes or interpolations, and the potential for few-shot learning or manipulations based on small data. However, we observed that, for voice conversion, results following this strategy were largely unsatisfactory (Appendix B).

Instead of using $\mathbf{z}$ to perform identity manipulations, we think of it as an identity-agnostic representation. Our idea is that any supplied condition specifying some real input characteristic of $\mathbf{x}$ should be useful to transform $\mathbf{x}$ to $\mathbf{z}$, specially if we consider a maximum likelihood objective. That is, knowing

a condition/characteristic of the input should facilitate the discovery of further similarities that were hidden by said condition/characteristic, and thus facilitate learning. Following this line of thought, if conditioning at multiple levels in the flow from $\mathbf{x}$ to $\mathbf{z}$ progressively get us to a condition-free $\mathbf{z}$ space (Appendix C.3), then, when transforming back from $\mathbf{z}$ to $\mathbf{x}$ with a different condition, that should also progressively imprint the characteristics of this new condition to the output $\mathbf{x}$. Blow uses the source speaker identifier y_{S} for transforming $\mathbf{x}^{(\mathrm{S})}$ to $\mathbf{z}$, and the target speaker identifier y_{T} for transforming $\mathbf{z}$ to the converted audio frame $\mathbf{x}^{(\mathrm{T})}$.

4.4 Hyperconditioning

A straightforward place to introduce conditioning in flow-based models is the coupling network, as no Jacobian matrix needs to be computed and no invertibility constraints apply. Furthermore, in the case of affine channel-wise couplings [16, 25], the coupling network is in charge of performing most of the transformation, so we want it to have a great representation power, possibly boosted by further conditioning information. A common way to condition the coupling network is to add or concatenate some representation to its input layers. However, based on our observations that concatenation tended to be ignored and that addition was not powerful enough, we decided to perform conditioning directly with the weights of the convolutional kernels. That is, that a conditioning representation determines the weights employed by a convolution operator, like done with hypernetworks [17]. We do it at the first layer of the coupling network (Fig. 1, right).

Using one-dimensional convolutions, and given an input activation matrix $\mathbf{H}$, for the i-th convolutional filter we have

$$\mathbf{h}^{(i)} = \mathbf{W}_y^{(i)} * \mathbf{H} + b_y^{(i)}, \tag{2}$$

where $*$ is the one-dimensional convolution operator, and $\mathbf{W}_y^{(i)}$ and $b_y^{(i)}$ represent the i-th kernel weights and bias, respectively, imposed by condition y. A set of n condition-dependent kernels and biases $\mathcal{K}_y$ can be obtained by

$$\mathcal{K}_y = \left\{ \left(\mathbf{W}_y^{(1)}, b_y^{(1)} \right) \dots \left(\mathbf{W}_y^{(n)}, b_y^{(n)} \right) \right\} = g\left(\mathbf{e}_y \right), \tag{3}$$

where g is an adapter network that takes the conditioning representation $\mathbf{e}_y$ as input, which in turn depends on condition identifier y (the speaker identity in our case). Vector $\mathbf{e}_y$ is an embedding that can either be fixed or initialized at some pre-calculated feature representation of a speaker, or learned from scratch if we need a standalone model. In this paper we choose the standalone version.

4.5 Structure-wise shared embeddings

We find that learning one $\mathbf{e}_y$ per coupling network usually results in sub-optimal results. We hypothesize that, given a large number of steps of flow (or coupling networks), independent conditioning representations do not need to focus on the essence of the condition (the speaker identity), and are thus free to learn any combination of numbers that minimizes the negative log-likelihood, irrespective of their relation with the condition. Therefore, to reduce the freedom of the model, we decide to constrain such representations. Loosely inspired by the StyleGAN architecture [46], we set a single learnable embedding $\mathbf{e}_y$ that is shared by each coupling network in all steps of flow (Fig. 1, left). This reduces both the number of parameters and the freedom of the model, and turns out to yield better results. Following a similar reasoning, we also use the smallest possible adapter network g (Fig. 1, right): a single linear layer with bias that merely performs dimensonality adjustment.

4.6 Data augmentation

To train Blow, we discard silent frames (Appendix B) and then enhance the remaining ones with 4 data augmentation strategies. Firstly, we apply a temporal jitter. We shift the start j of each frame $\mathbf{x}$ as $j' = j + \lfloor U(-\xi, \xi) \rceil$, where U is a uniform random number generator and ξ is half of the frame size. Secondly, we use a random pre-/de-emphasis filter. Since the identity of the speaker is not going to vary with a simple filtering strategy, we apply an emphasis filter [47] with a coefficient $\alpha = U(-0.25, 0.25)$. Thirdly, we perform a random amplitude scaling. Speaker identity is also going to be preserved with scaling, plus we want the model to be able to deal with any amplitude between -1 and 1. We use $\mathbf{x}' = U(0, 1) \cdot \mathbf{x} / \max(|\mathbf{x}|)$. Finally, we randomly flip the values in the frame. Auditory perception is relative to an average pressure level, so we can flip the sign of $\mathbf{x}$ to obtain a different input with the same perceptual qualities: $\mathbf{x}' = \mathrm{sgn}(U(-1, 1)) \cdot \mathbf{x}$.

4.7 Implementation details

We now outline the details that differ from the common implementation of flow-based generative models and further refer the interested reader to the provided code for a full account of them. We also want to note that we did not perform any hyperparameter tuning on Blow.

General — We train Blow with Adam using a learning rate of 10^{-4} and a batch size of 114. We anneal the learning rate by a factor of 5 if 10 epochs have passed without improvement in the validation set, and stop training at the third time this happens. We use an 8×12 structure, with $2\times$ alternate-pattern squeezing operations. For the coupling network, we split channels into two halves, and use one-dimensional convolutions with 512 filters and kernel widths 3, 1, and 3. Embeddings are of dimension 128. We train with a frame size of 4096 at 16 kHz with no overlap, and initialize the ActNorm weights with one data-augmented batch (batches contain a random mixture of frames from all speakers). We synthesize with a Hann window and 50% overlap, normalizing the entire utterance between -1 and 1. We implement Blow using PyTorch [48].

Coupling — As done in the official Glow code (but not mentioned in the paper), we find that constraining the scaling factor that comes out of the coupling network improves the stability of training. For affine couplings with channel-wise concatenation

$$\mathbf{H}' = \left[\ \mathbf{H}_{1:c}\ ,\ s'(\mathbf{H}_{1:c})\,(\mathbf{H}_{c+1:2c} + t(\mathbf{H}_{1:c}))\ \right],$$

where $2c$ is the total number of channels, we use

$$s'(\mathbf{H}_{1:c}) = \sigma(s(\mathbf{H}_{1:c}) + 2) + \epsilon,$$

where σ corresponds to the sigmoid function and ϵ is a small constant to prevent an infinite log-determinant (and division by 0 in the reverse pass).

Hyperconditioning — If we strictly follow Eqs. 2 and 3, the hyperconditioning operation can involve both a large GPU memory footprint (n different kernels per batch element) and time-consuming calculations (a double loop for every kernel and batch element). This can, in practice, make the operation impossible to perform for a very deep flow-based architecture like Blow. However, by restricting the dimensionality of kernels $\mathbf{W}_y^{(i)}$ such that every channel is convolved with its own set of kernels, we can achieve a minor GPU footprint and a tractable number of parameters per adaptation network. This corresponds to depthwise separable convolutions [49], and can be implemented with grouped convolution [50], available in most deep learning libraries.

5 Experimental setup

To study the performance of Blow we use the VCTK data set [51], which comprises 46 h of audio from 109 speakers. We downsample it at 16 kHz and randomly extract 10% of the sentences for validation and 10% for testing (we use a simple parsing script to ensure that the same sentence text does not get into different splits, see Appendix B). With this amount of data, the training of Blow takes 13 days using three GeForce RTX 2080-Ti GPUs[1]. Conversions are performed between all possible gender combinations, from test utterances to randomly-selected VCTK speakers.

To compare with existing approaches, we consider two flow-based generative models and two competitive voice conversion systems. As flow-based generative models we adapt Glow [16] to the one-dimensional case and replicate a version of Glow with a WaveNet coupling network following [6, 7] (Glow-WaveNet). Conversion is done both via manipulation of the $\mathbf{z}$ space and by learning an identity conditioner (Appendix B). These models use the same frame size and have the same number of flow steps as Blow, with a comparable number of parameters. As voice conversion systems we implement a VQ-VAE architecture with a WaveNet decoder [33] and an adaptation of the StarGAN architecture to voice conversion like StarGAN-VC [14]. VQ-VAE converts in the waveform domain, while StarGAN does it between mel-cepstrums. Both systems can be considered as very competitive for the non-parallel voice conversion task. We do not use pre-training nor transfer learning in any of the models.

To quantify performance, we carry out both objective and subjective evaluations. As objective metrics we consider the per-dimensionality log-likelihood of the flow-based models (L) and a spoofing

[1]Nonetheless, conversion plus synthesis with 1 GPU and 50% overlap is around $14\times$ faster than real time.

Table 1: Objective scores and their relative difference for possible Blow alternatives (5 min per speaker, 100 epochs).

Configuration	L [nat/dim]	Spoofing [%]
Blow	**4.30**	**66.2**
1: with 3×32 structure	4.01 (− 6.7%)	17.2 (−74.0%)
2: with 3×32 structure (squeeze of 8)	4.21 (− 2.1%)	65.7 (− 0.8%)
3: with multi-scale structure	3.64 (−15.3%)	3.5 (−94.7%)
4: with multi-scale structure (5×19, squeeze of 4)	3.99 (− 7.2%)	16.6 (−74.9%)
5: with additive conditioning (coupling network)	4.28 (− 0.5%)	39.5 (−40.3%)
6: with additive conditioning (before ActNorm)	4.28 (− 0.5%)	22.5 (−66.0%)
7: without data augmentation	4.15 (− 3.5%)	28.3 (−57.2%)

Table 2: Objective and subjective voice conversion scores. For all measures, higher is better. The first two reference rows correspond to using original recordings from source or target speakers as target.

Approach	Objective		Subjective	
	L [nat/dim]	Spoofing [%]	Naturalness [1–5]	Similarity [%]
Source as target	n/a	1.1	4.83	10.6
Target as target	n/a	99.3	4.83	98.5
Glow	4.11	1.2	n/a	n/a
Glow-WaveNet	4.18	3.1	n/a	n/a
StarGAN	n/a	44.4	**2.87**	61.8
VQ-VAE	n/a	65.0	2.42	69.7
Blow	**4.45**	**89.3**	2.83	**77.6**

measure reflecting the percentage of times a conversion is able to fool a speaker identification classifier (Spoofing). The classifier is an MFCC-based single-layer classifier trained with the same split as the conversion systems (Appendix B). For the subjective evaluation we follow Wester et al. [52] and consider the naturalness of the speech (Naturalness) and the similarity of the converted speech to the target identity (Similarity). Naturalness is based on a mean opinion score from 1 to 5, while Similarity is an aggregate percentage from a binary rating. A total of 33 people participated in the subjective evaluation. Further details on our experimental setup are given in Appendix B.

6 Results

6.1 Ablation study

First of all, we assess the effect of the introduced changes with objective scores L and Spoofing. Due to computational constraints, in this set of experiments we limit training to 5 min of audio per speaker and 100 epochs. The results are in Table 1. In general, we see that all introduced improvements are important, as removing any of them always implies worse scores. Nonetheless, some are more critical than others. The most critical one is the use of a single-scale structure. The two alternatives with a multi-scale structure (3–4) yield the worst likelihoods and spoofings, to the point that (3) does not even perform any conversion. Using an 8×12 structure instead of the original 3×32 structure of Glow can also have a large effect (1). However, if we further tune the squeezing factor we can mitigate it (2). Substituting the hyperconditioning module by a regular convolution plus a learnable additive embedding has a marginal effect on L, but a crucial effect on Spoofing (5–6). Finally, the proposed data augmentation strategies also prove to be important, at least with 5 min per speaker (7).

6.2 Voice conversion

In Table 2 we show the results for both objective and subjective scores. The two objective scores, L and Spoofing, indicate that Blow outperforms the other considered approaches. It achieves a relative L increment of 6% from Glow-Wavenet and a relative Spoofing increment of 37% from VQ-VAE. Another thing to note is that adapted Glow-based models, although achieving a reasonable likelihood,

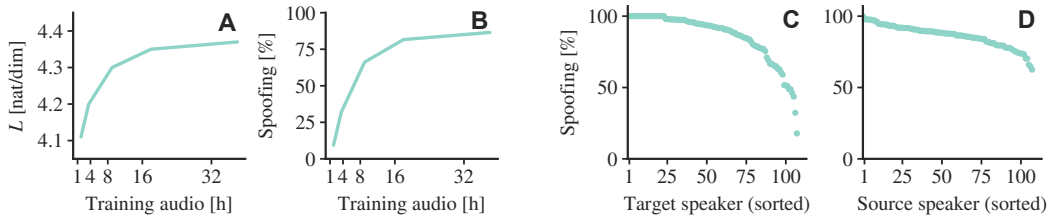


Figure 2: Objective scores with respect to amount of training (A–B) and target/source speaker (C–D).

are not able to perform conversion, as their Spoofing is very close to that of the "source as target" reference. Because of that, we discarded those in the subjective evaluation.

The subjective evaluation confirms the good performance of Blow. In terms of Naturalness, StarGAN outperforms Blow, albeit by only a 1% relative difference, without statistical significance (ANOVA, $p = 0.76$). However, both approaches are significantly below the reference audios ($p < 0.05$). In terms of similarity to the target, Blow outperforms both StarGAN and VQ-VAE by a relative 25 and 11%, respectively. Statistical significance is observed between Blow and StarGAN (Barnard's test, $p = 0.02$) but not between Blow and VQ-VAE ($p = 0.13$). Further analysis of the obtained subjective scores can be found in Appendix C. To put Blow's results into further perspective, we can have a look at the non-parallel task of the last voice conversion challenge [10], where systems that do not perform transfer learning or pre-training achieve Naturalness scores slightly below 3.0 and Similarity scores equal to or lower than 75%. Example conversions can be listened from `https://blowconversions.github.io`.

6.3 Amount of training data and source/target preference

To conclude, we study the behavior of the objective scores when decreasing the amount of training audio (including the inherent silence in the data set, which we estimate is around 40%). We observe that, at 100 epochs, training with 18 h yields almost the same likelihood (Fig. 2A) and spoofing (Fig. 2B) than training with the full set of 37 h. With it, we do not observe any clear relationship between Spoofing and per-speaker duration (Appendix C). What we observe, however, is a tendency with regard to source and target identities. If we average spoofing scores for a given target identity, we obtain both almost-perfect scores close to 100% and some scores below 50% (Fig. 2C). In contrast, if we average spoofing scores for a given source identity, those are almost always above 70% and below 100% (Fig. 2D). This indicates that the target identity is critical for the conversion to succeed, with relative independence of the source. We hypothesize that this is due to the way normalizing flows are trained (maximizing likelihood only for single inputs and identifiers; never performing an actual conversion to a target speaker), but leave the analysis of this phenomenon for future work.

7 Conclusion

In this work we put forward the potential of flow-based generative models for raw audio synthesis, and specially for the challenging task of non-parallel voice conversion. We propose Blow, a single-scale hyperconditioned flow that features a many-block structure with shared embeddings and performs conversion in a forward-backward manner. Because Blow departs from existing flow-based generative models in these aspects, it is able to outperform those and compete with, or even improve upon, existing non-parallel voice conversion systems. We also quantify the impact of the proposed improvements and assess the effect that the amount of training data and the selection of source/target speaker can have in the final result. As future work, we want to improve the model to see if we can deal with other tasks such as speech enhancement or instrument conversion, perhaps by further enhancing the hyperconditioning mechanism or, simply, by tuning its structure or hyperparameters.

Acknowledgments

We are grateful to all participants of the subjective evaluation for their input and feedback. We thank Antonio Bonafonte, Ferran Diego, and Martin Pielot for helpful comments. SP acknowledges partial support from the project TEC2015-69266-P (MINECO/FEDER, UE).

References

[1] A. Van den Oord, S. Dieleman, H. Zen, K. Simonyan, O. Vinyals, A. Graves, N. Kalchbrenner, A. Senior, and K. Kavukcuoglu. WaveNet: a generative model for raw audio. *ArXiv*, 1609.03499, 2016.

[2] S. Mehri, K. Kumar, I. Gulrajani, R. Kumar, S. Jain, J. Sotelo, A. Courville, and Y. Bengio. SampleRNN: an unconditional end-to-end neural audio generation model. In *Proc. of the Int. Conf. on Learning Representations (ICLR)*, 2017.

[3] N. Kalchbrenner, E. Elsen, K. Simonyan, N. Casagrande, E. Lockhart, F. Stimberg, A. Van den Oord, S. Dieleman, and K. Kavukcuoglu. Efficient neural audio synthesis. In *Proc. of the Int. Conf. on Machine Learning (ICML)*, pages 2410–2419, 2018.

[4] S. Pascual, A. Bonafonte, and J. Serrà. SEGAN: speech enhancement generative adversarial network. In *Proc. of the Int. Speech Communication Association Conf. (INTERSPEECH)*, pages 3642–3646, 2017.

[5] C. Donahue, J. McAuley, and M. Puckette. Adversarial audio synthesis. In *Proc. of the Int. Conf. on Learning Representations (ICLR)*, 2019.

[6] R. Prenger, R. Valle, and B. Catanzaro. WaveGlow: a flow-based generative network for speech synthesis. In *Proc. of the IEEE Int. Conf. on Acoustics, Speech and Signal Processing (ICASSP)*, pages 3617–3621, 2018.

[7] S. Kim, S.-G. Lee, J. Song, and S. Yoon. FloWaveNet : a generative flow for raw audio. In *Proc. of the Int. Conf. on Machine Learning (ICML)*, pages 3370–3378, 2018.

[8] S. Dieleman, A. Van den Oord, and K. Simonyan. The challenge of realistic music generation: modeling raw audio at scale. In *Advances in Neural Information Processing Systems (NeurIPS)*, volume 31, pages 7989–7999. Curran Associates, Inc., 2018.

[9] S. H. Mohammadi and A. Kain. An overview of voice conversion systems. *Speech Communication*, 88:65–82, 2017.

[10] J. Lorenzo-Trueba, J. Yamagishi, T. Toda, D. Saito, F. Villavicencio, T. Kinnunen, and Z. Ling. The voice conversion challenge 2018: promoting development of parallel and nonparallel methods. In *Proc. of Odissey, The Speaker and Language Recognition Workshop (Odissey)*, pages 195–202, 2018.

[11] Y. Saito, Y. Ijima, K. Nishida, and S. Takamichi. Non-parallel voice conversion using variational autoencoders conditioned by phonetic posteriorgrams and d-vectors. In *Proc. of the IEEE Int. Conf. on Acoustics, Speech and Signal Processing (ICASSP)*, pages 5274–5278, 2018.

[12] H. Kameoka, T. Kaneko, K. Tanaka, and N. Hojo. ACVAE-VC: Non-parallel many-to-many voice conversion with auxiliary classifier variational autoencoder. *ArXiv*, 1808.05092, 2018.

[13] T. Kaneko and H. Kameoka. CycleGAN-VC: non-parallel voice conversion using cycle-consistent adversarial networks. In *Proc. of the European Signal Processing Conf. (EUSIPCO)*, pages 2114–2118, 2018.

[14] H. Kameoka, T. Kaneko, K. Tanaka, and N. Hojo. StarGAN-VC: non-parallel many-to-many voice conversion with star generative adversarial networks. In *Proc. of the IEEE Spoken Language Technology Workshop (SLT)*, pages 266–273, 2018.

[15] C. C. Hsu, H. T. Hwang, Y. C. Wu, Y. Tsao, and H. M. Wang. Voice conversion from unaligned corpora using variational autoencoding wasserstein generative adversarial networks. In *Proc. of the Int. Speech Communication Association Conf. (INTERSPEECH)*, pages 3364–3368, 2017.

[16] D. P. Kingma and P. Dhariwal. Glow: generative flow with invertible 1x1 convolutions. In *Advances in Neural Information Processing Systems (NeurIPS)*, volume 31, pages 10215–10224. Curran Associates, Inc., 2018.

[17] D. Ha, A. Dai, and Q. V. Le. HyperNetworks. In *Proc. of the Int. Conf. on Learning Representations (ICLR)*, 2017.

[18] M. Yamaguchi, Y. Koizumi, and N. Harada. AdaFlow: domain-adaptive density estimator with application to anomaly detection and unpaired cross-domain translation. In *Proc. of the IEEE Int. Conf. on Acoustics, Speech and Signal Processing (ICASSP)*, pages 3647–3651, 2019.

[19] Y. Li, N. Wang, J. Shi, H. Hou, and J. Liu. Adaptive batch normalization for practical domain adaptation. *Pattern Recognition*, 80:109–117, 2018.

[20] H. B. Barlow. Unsupervised learning. *Neural Computation*, 1:295–311, 1989.

[21] A. N. Redlich. Supervised factorial learning. *Neural Computation*, 5:750–766, 1993.

[22] G. Deco and W. Brauer. Higher order statistical decorrelation without information loss. In *Advances in Neural Information Processing Systems (NeurIPS)*, volume 7, pages 247–254. MIT Press, 1995.

[23] L. Dinh, D. Krueger, and Y. Bengio. NICE: non-linear independent components estimation. In *Proc. of the Int. Conf. on Learning Representations (ICLR)*, 2015.

[24] D. J. Rezende and S. Mohamed. Variational inference with normalizing flows. In *Proc. of the Int. Conf. on Machine Learning (ICML)*, pages 1530–1538, 2015.

[25] L. Dinh, J. Sohl-Dickstein, and S. Bengio. Density estimation using Real NVP. In *Proc. of the Int. Conf. on Learning Representations (ICLR)*, 2017.

[26] E. G. Tabak and C. V. Turner. A family of non-parametric density estimation algorithms. *Communications on Pure and Applied Mathematics*, 66(2):145–164, 2013.

[27] A. Mouchtaris, J. Van der Spiegel, and P. Mueller. Non-parallel training for voice conversion based on a parameter adaptation approach. *IEEE Trans. on Audio, Speech and Language Processing*, 14(3):952–963, 2006.

[28] D. Erro, A. Moreno, and A. Bonafonte. INCA algorithm for training voice conversion systems from nonparallel corpora. *IEEE Trans. on Audio, Speech and Language Processing*, 18(5): 944–953, 2010.

[29] Z. Wu, T. Kinnunen, E. S. Chang, and H. Li. Mixture of factor analyzers using priors from non-parallel speech for voice conversion. *IEEE Signal Processing Letters*, 19(12):914–917, 2012.

[30] T. Kinnunen, L. Juvela, P. Alku, and J. Yamagishi. Non-parallel voice conversion using i-vector PLDA: towards unifying speaker verification and transformation. In *Proc. of the IEEE Int. Conf. on Acoustics, Speech and Signal Processing (ICASSP)*, pages 5535–5539, 2017.

[31] F.-L. Xie, F. K. Soong, and H. Li. A KL divergence and DNN-based approach to voice conversion without parallel training sentences. In *Proc. of the Int. Speech Communication Association Conf. (INTERSPEECH)*, pages 287–291, 2016.

[32] S. O. Arik, J. Chen, K. Peng, W. Ping, and Y. Zhou. Neural voice cloning with a few samples. In *Advances in Neural Information Processing Systems (NeurIPS)*, volume 31, pages 10019–10029. Curran Associates, Inc., 2018.

[33] A. Van den Oord, O. Vinyals, and K. Kavukcuoglu. Neural discrete representation learning. In *Advances in Neural Information Processing Systems (NeurIPS)*, volume 30, pages 6306–6315. Curran Associates, Inc., 2017.

[34] J. Engel, C. Resnick, A. Roberts, S. Dieleman, D. Eck, K. Simonyan, and M. Norouzi. Neural audio synthesis of musical notes with WaveNet autoencoders. In *Proc. of the Int. Conf. on Machine Learning (ICML)*, pages 1068–1077, 2017.

[35] N. Mor, L. Wolf, A. Polyak, and Y. Taigman. A universal music translation network. In *Proc. of the Int. Conf. on Learning Representations (ICLR)*, 2019.

[36] E. Nachmani and L. Wolf. Unsupervised singing voice conversion. *ArXiv*, 1904.06590, 2019.

[37] A. Haque, M. Guo, and P. Verma. Conditional end-to-end audio transforms. In *Proc. of the Int. Speech Communication Association Conf. (INTERSPEECH)*, pages 2295–2299, 2018.

[38] W. Grathwohl, R. T. Q. Chen, J. Bettencourt, I. Sutskever, and D. Duvenaud. FFJORD: free-form continuous dynamics for scalable reversible generative models. In *Proc. of the Int. Conf. on Learning Representations (ICLR)*, 2019.

[39] J. Ho, X. Chen, A. Srinivas, R. Duan, and P. Abbeel. Flow++: improving flow-based generative models with variational dequantization and architecture design. In *Proc. of the Int. Conf. on Machine Learning (ICML)*, pages 2722–2730, 2019.

[40] L. Dinh, J. Sohl-Dickstein, R. Pascanu, and H. Larochelle. A RAD approach to deep mixture models. *ArXiv*, 1903.07714, 2019.

[41] M. Livne and D. J. Fleet. TzK Flow - Conditional Generative Model. *ArXiv*, 1811.01837, 2018.

[42] S. J. Hwang and W. H. Kim. Conditional recurrent flow: conditional generation of longitudinal samples with applications to neuroimaging. *ArXiv*, 1811.09897, 2018.

[43] E. Hoogeboom, R. Van den Berg, and M. Welling. Emerging convolutions for generative normalizing flows. In *Proc. of the Int. Conf. on Machine Learning (ICML)*, pages 2771–2780, 2019.

[44] K. Simonyan and A. Zisserman. Very deep convolutional networks for large-scale image recognition. In *Proc. of the Int. Conf. on Learning Representations (ICLR)*, 2015.

[45] B. Ziolko and M. Ziolko. Time durations of phonemes in Polish language for speech and speaker recognition. In Z. Vetulani, editor, *Human language technology - Challenges for computer science and linguistics*, volume 6562 of *Lecture Notes in Computer Science*. Springer, Berlin, Germany, 2011.

[46] T. Karras, S. Laine, and T. Aila. A style-based generator architecture for generative adversarial networks. In *Proc. of the Conf. on Computer Vision and Pattern Recognition (CVPR)*, 2019.

[47] P. Boersma and D. Weenink. Praat: doing phonetics by computer, 2019. URL http://www.praat.org/.

[48] A. Paszke, S. Gross, S. Chintala, G. Chanan, E. Yang, Z. DeVito, Z. Lin, A. Desmaison, L. Antiga, and A. Lerer. Automatic differentiation in PyTorch. In *NeurIPS Workshop on The Future of Gradient-based Machine Learning Software & Techniques (NeurIPS-Autodiff)*, 2017.

[49] L. Kaiser, A. N. Gomez, and F. Chollet. Depthwise separable convolutions for neural machine translation. In *Proc. of the Int. Conf. on Learning Representations (ICLR)*, 2018.

[50] A. Krizhevsky, I. Sutskever, and G. Hinton. ImageNet classification with deep convolutional neural networks. In *Advances in Neural Information Processing Systems (NeurIPS)*, volume 25, pages 1097–1105. Curran Associates, Inc., 2012.

[51] C. Veaux, J. Yamagishi, and K. MacDonald. CSTR VCTK corpus: English multi-speaker corpus for CSTR voice cloning toolkit, 2012. URL http://dx.doi.org/10.7488/ds/1994.

[52] M. Wester, Z. Wu, and J. Yamagishi. Analysis of the voice conversion challenge 2016 evaluation results. In *Proc. of the Int. Speech Communication Association Conf. (INTERSPEECH)*, pages 1637–1641, 2016.

[53] Y. Choi, M. Choi, M. Kim, J.-W. Ha, S. Kim, and J. Choo. StarGAN: unified generative adversarial networks for multi-domain image-to-image translation. In *Proc. of the Conf. on Computer Vision and Pattern Recognition (CVPR)*, pages 8789–8797, 2018.

[54] M. Morise, F. Yokomori, and K. Ozawa. WORLD: a vocoder-based high-quality speech synthesis system for real-time applications. *IEICE Transactions on Information and Systems*, 99(7):1877–1884, 2016.

[55] S. O. Arik, M. Chrzanowski, A. Coates, G. Diamos, A. Gibiansky, Y. Kang, X. Li, J. Miller, A. Ng, J. Raiman, S. Sengupta, and M. Shoeybi. Deep voice: real-time neural text-to-speech. In *Proc. of the Int. Conf. on Machine Learning (ICML)*, pages 195–204, 2017.

Appendix

A Recap of the log-likelihood equation derivation

Following Rezende and Mohamed [24], if we use a normalizing flow f to transform a random variable $\mathbf{x}$ with distribution $p(\mathbf{x})$, the resulting random variable $\mathbf{z} = f(\mathbf{x})$ has a distribution

$$p\left(\mathbf{z}\right) = p\left(f\left(\mathbf{x}\right)\right) = p\left(\mathbf{x}\right)\left|\det\left(\frac{\partial f^{-1}(\mathbf{z})}{\partial \mathbf{z}}\right)\right|,$$

which is derived from the change of variables formula. By the inverse function theorem, we can work with the Jacobian of f,

$$p\left(\mathbf{z}\right) = p\left(\mathbf{x}\right)\left|\det\left(\frac{\partial f(\mathbf{z})}{\partial \mathbf{z}}\right)\right|^{-1}$$

and, taking logarithms and rearranging, we reach

$$\log\left(p\left(\mathbf{x}\right)\right) = \log\left(p\left(\mathbf{z}\right)\right) + \log\left|\det\left(\frac{\partial f(\mathbf{z})}{\partial \mathbf{z}}\right)\right|,$$

as expressed by, for instance, Dinh et al. [25]. Finally, since f is a composite function (Sec. 3), we can write the previous equation as Kingma and Dhariwal [16]:

$$\log\left(p\left(\mathbf{x}\right)\right) = \log\left(p\left(\mathbf{z}\right)\right) + \sum_{i=1}^{k}\log\left|\det\left(\frac{\partial f_i(\mathbf{h}_{i-1})}{\partial \mathbf{h}_{i-1}}\right)\right|.$$

This is the expression we use to optimize the normalizing flow. Notice that log-determinants can be factored out at each flow step, shuttling gradients back to each f_i (or $\mathbf{h}_i$) and below.

B Detail of the experimental setup

B.1 Data

As mentioned in the main paper, we use the VCTK data set [51], which originally contains 46 h of audio from 109 speakers. The only pre-processing we perform to the original audio is to downsample to 16 kHz and to normalize every file between -1 and 1. Later, at training time, silent frames with a standard deviation below 0.025 are discarded. As mentioned, we use frames of 4096 samples.

To obtain train, validation, and test splits, we parse the text of every sentence and group utterances of the same text (we discard the speaker without available text). We then randomly extract 10% of the sentences for validation and 10% for test. This way, we force that the same text content is not present in more than one split, and therefore that sentences in validation or test are not included in training. The total amount of training audio is 36 h which, with 108 speakers, yields an average of 20 min per speaker. Other statistics are reported in Table 3.

Table 3: Train, validation, and test numbers.

Description	Train	Validation	Test
Audio duration	36.7 h	4.4 h	4.5 h
Number of sentences	10609	1325	1325
Number of files	35247	4417	4406
Number of frames (discarding silence)	291154	34390	35253

All reported results are based on the test split, including the audios used for subjective evaluation. We perform one conversion per test file, by choosing a different speaker from the pool of all available speakers uniformly at random (irrespective of the gender or other metadata).

B.2 Baselines

B.2.1 Glow-based

For performing audio conversion with Glow-based baselines, we initially considered a conditioning-only strategy. In the case of Glow, this implied computing a Gaussian mean for every label at training time and subtracting it in $\mathbf{z}$ space (adding it when going from $\mathbf{z}$ to $\mathbf{x}$). In the case of Glow-WaveNet, as it directly accepts a conditioning, we implement independent learnable embeddings that are added at the first layer of every coupling, as done with the mel conditioning of WaveGlow [6]. The conditioning-only strategy, however, turned out to perform poorly for these models in preliminary experiments.

Using a manipulation-only strategy as proposed by Kingma and Dhariwal [16] was also found to perform poorly. Some conversion could be perceived, like for instance changing identities from male to female, but obtained identities were not similar to the target ones. In addition, we found annoying audio artifacts were easily appearing, and that those could be amplified with just minimal changes in the manipulation strategy.

In the end, we decided to use both strategies and augment the conditioning-only strategy with the semantic manipulation one. We empirically chose a scaling factor of 3 as a trade-off between amount of conversion and generation of artifacts. We also found that weighting the contribution to the mean by the energy of $\mathbf{x}$ could slightly improve conversion.

B.2.2 StarGAN

The baseline StarGAN model is based on StarGAN-VC [14], which uses StarGAN [53] to learn non-parallel many-to-many mappings between speakers. It is worth noting that this approach does not work at the waveform level, but instead extracts the fundamental frequency, aperiodicity, and spectral envelope from each audio clip, and then performs the conversion by means of its generator at the spectral envelope level. For generating the target speakers' speech, the WORLD vocoder [54] is used with the transformed spectral envelope, linearly-converted pitch, and original aperiodicity as inputs.

In the original StarGAN-VC paper, the experiments comprised only 4 speakers (2 male and 2 female), while in this work we extended it to all VCTK speakers. However, in our setup, publicly available implementations of this architecture did not generate a reasonably natural speech, and hence we tried with a alternative implementation. In particular, our baseline is based on an implementation[2] that uses the same architecture as the original image-to-image StarGAN [53]. The main difference with StarGAN-VC is that it does not include any conditioning on the speaker in the discriminator network, but instead the discriminator and domain classifier (that acts as a speaker classifier) share the same underlying network weights. The other difference is that the training uses a Wasserstein GAN objective with gradient penalty.

B.2.3 VQ-VAE

The baseline VQ-VAE model for voice conversion is based on [33]. The exact specification details such as the waveform encoder architecture are not provided in the paper and, to our knowledge, an official model implementation has not been published so far. We tried a number of non-official implementations but, in the end, found our own implementation to perform better in preliminary experiments.

Our implementation follows as closely as possible [33]. We use 7 strided convolutions for the audio encoder with a stride of 2 and a kernel size of 4, with 448 channels in the last layer. Therefore, we have a time-domain compression of 2^7 compared to the original raw audio. The feature map is then projected into a latent space of dimension 128, and the discrete space of the quantized vectors is 512. The discrete latent codes are concatenated with the target speaker embedding and then upsampled in the time dimension using a deconvolutional layer with a stride of 2^7, which is used as the local conditioning for the WaveNet decoder. To speed up the audio generation, our WaveNet implementation uses the one provided by NVIDIA[3], which implements the WaveNet variant

[2] https://github.com/liusongxiang/StarGAN-Voice-Conversion

[3] https://github.com/NVIDIA/nv-wavenet

described by Arik et al. [55]. However, to perform a fair comparison with Blow (and possibly differently from [33]), we do not use any pre-trained weight in the WaveNet nor the VQ-VAE structures.

B.3 Spoofing classifier

To objectively evaluate the capacity of the considered approaches to perform voice conversion we employ a speaker identity classifier, which we train on the same split as the conversion approaches. The classifier uses classic speech features computed within a short-time frame. With that, we believe the Spoofing measure captures not only speaker identities, but can also be affected by audio artifacts or distortions that may have an impact to the short-time, frame-based features. We use 40 mel-frequency cepstral coefficients (MFCCs), their deltas, their delta-deltas, and the root mean square energy. From those we then compute the mean and the standard deviation across frames to summarize the speaker identity in an audio file. To extract features we use librosa[4] with default parameters, except for some of the MFCC ones: FFT hop of 128, FFT window of 256, FFT size of 2048, and 200 mel bands. After feature extraction, we apply z-score normalization, computing the mean and the standard deviation from training data.

The classifier is a linear network with dropout, trained with categorical cross-entropy. We then apply a dropout of 0.4 to the input features and a linear layer with bias. We train the classifier with Adam using a learning rate of 10^{-3} and stop training when the validation loss has not improved for 10 epochs. With 108 speakers, this classifier achieves an accuracy of 99.3% on the test split.

B.4 Subjective evaluation

For the subjective evaluation we follow Wester et al. [52]. They divide it into two aspects: naturalness and similarity. Naturalness aims to measure the amount of artifacts or distortion that is present in the generated signals. Similarity aims to measure how much the converted speaker identity resembles either the source or the target identity. Naturalness is measured with a mean opinion score between 1 and 5, and similarities are measured with a binary decision, allowing the option to express some uncertainty. Statistical significance is assessed with an analysis of variance (ANOVA) for Naturalness and with Barnard's test for Similarity (both single tail, with $p < 0.05$).

A total of 33 subjects participated of the subjective evaluation. From those, 3 were native English speakers and 8 declared having some speech processing expertise. Participants were presented to 16 audio examples in the Naturalness assessment part (4 per system) and to 16 audio pairs in the Similarity assessment part (4 per system, two for similar to the target and two for similar to the source assessments).

C Additional results

C.1 Analysis of subjective scores

A visual summary of the numbers reported in the main paper is depicted in Fig. 3. We see that the three considered systems cluster together, falling apart from the real target and source voices. Among the three systems, Blow stands out, specially in similarity to the target (vertical axis), and competes closely with StarGAN in terms of Naturalness (horizontal axis).

If we study naturalness scores alone, we see that the difference between Blow and StarGAN is minimal (Fig 4). Actually, we find no statistically significant difference between the two (ANOVA, $p = 0.76$). This is a good result if we consider that spectral-based approaches, such as StarGAN, are often preferred with regard to Naturalness due to their constriction to not generate audible artifacts in the time domain.

If we study similarity judgments alone, we observe a different picture (Figs. 5 and 6). Focusing on similarity to the target, Blow performs better than StarGAN and VQ-VAE. The ranking of the methods can be clearly seen when disregarding the confidence on the decisions (Fig. 5, left). Statistical significance is observed between Blow and StarGAN (Barnard's test, $p = 0.02$) but not between Blow and VQ-VAE ($p = 0.13$). If we consider the degree of confidence, we see the difference is in

[4] http://librosa.github.io/librosa

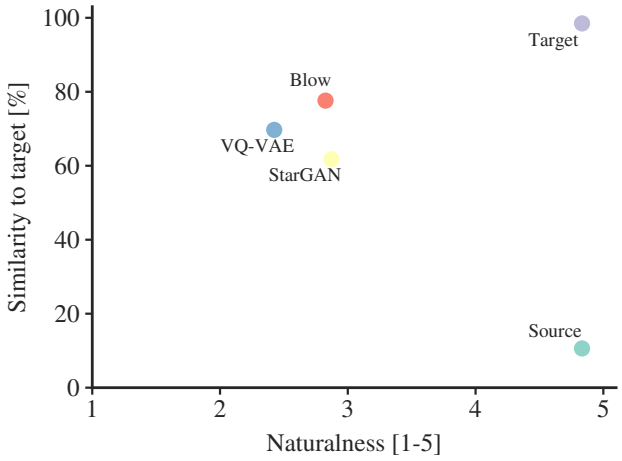


Figure 3: Scatter plot of the subjective evaluation results: Naturalness (horizontal axis) and similarity to the target (vertical axis) for the considered models and references.

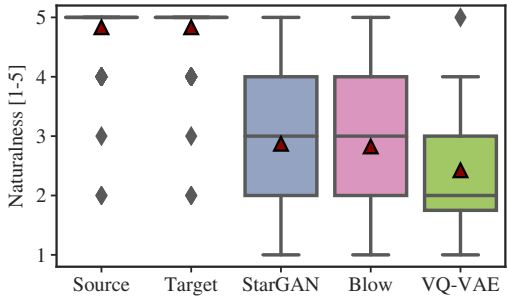


Figure 4: Box plot of Naturalness MOS. Red triangles indicate the arithmetic mean.

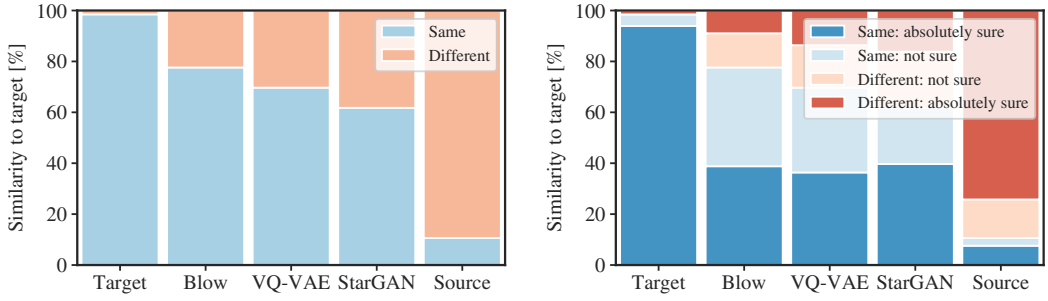


Figure 5: Similarity to the target ratings disregarding confidence (left) and including confidence assessment (right).

the "Same: not sure" ratings, as all three obtain almost the same number of "Same: absolutely sure" decisions (Fig. 5, right).

Finally, it is also interesting to look at the results for similarity to the source (Fig. 6). In them, we see that Blow and StarGAN generate slightly more audios that are considered to be similar to the source than VQ-VAE. This could indicate a problem in converting from some source identities, as the characteristics of those seem to remain in the conversion. However, in general, the amount of "Similar to the source" conversions is low, below 20%, and relatively close to the 10.6% obtained for the control group that compares real different identities (the target ones) with the source identities (Fig. 6, leftmost bars).

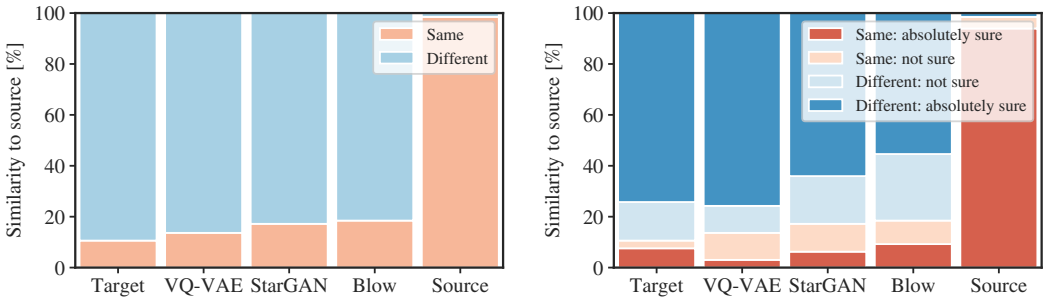


Figure 6: Similarity to the source ratings disregarding confidence (left) and including confidence (right) assessments.

Table 4: Objective scores at 100 epochs for different training sizes.

Total amount of training audio	1.8 h	3.6 h	9 h	18 h	37 h (full)
Training audio per speaker	1 min	2 min	5 min	10 min	20.4 min (average)
L [nat/dim]	4.11	4.20	4.30	4.35	4.37
Spoofing [%]	9.3	31.9	66.2	81.6	86.5

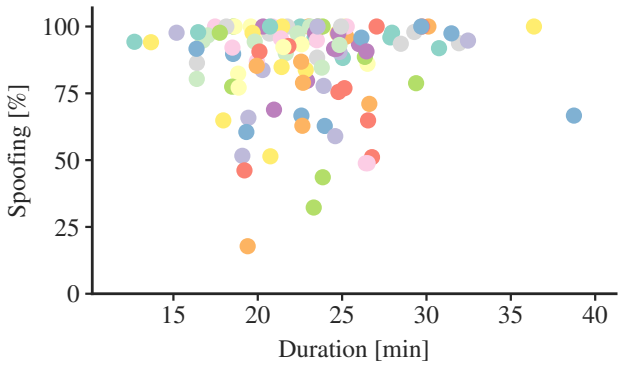


Figure 7: Spoofing percentage with respect to amount of training audio per speaker at 100 training epochs (full data set, including silence).

C.2 Amount of training audio

For completeness, in Table 4 we report the exact numbers depicted in Figs. 2A and 2B of the main paper. In Fig. 7, we further study Spoofing with respect to the amount of audio per speaker in the full training set. We do not observe any trend with respect to duration of training audio per speaker. All these results are calculated after 100 epochs of training.

C.3 Condition-free latent space

A driving idea of Blow is that the latent space $\mathbf{z}$ should be condition-free (or identity-agnostic). This is what motivates us to use hyperconditioning to progressively remove condition/identity characteristics when transforming from $\mathbf{x}$ to $\mathbf{z}$ (and later to progressively imprint new condition/identity characteristics when transforming back from $\mathbf{z}$ to $\mathbf{x}$). In order to substantiate a bit more our hypothesis, we decide to study the capacity to perform speaker identification in the latent space $\mathbf{z}$. The idea is that, if $\mathbf{z}$ vectors contain some speaker information, a classifier should be able to perform some speaker identification in $\mathbf{z}$ space.

To quantify the amount of speaker identity information present in $\mathbf{z}$, we proceed as with the Spoofing classifier (see above), but using the actual vectors $\mathbf{z}$ as frame-based features. The only difference is that, in the current case, we are interested in the result of a more complex classifier with enough power to extract non-trivial, relevant information from the features, if any. To this end, we consider a random forest classifier and a multi-layer perceptron (we use scikit-learn version 0.20.2 with default parameters, except for the number of estimators of the random forest classifier, which we set to 50, and the number of layers of the multi-layer perceptron, which we set to three, with 1000 and 100 intermediate activations).

The test accuracies we obtain for the two classifiers are 1.8% (random forest) and 1.4% (multi-layer perceptron). Both are only marginally above random chance (1.1%), and far from the value obtained by classic features extracted from $\mathbf{x}$ (99.3%). This gives us an indication that there is little identity information in the $\mathbf{z}$ space. However, to further confirm our original hypothesis, additional experiments on the latent space $\mathbf{z}$, which are beyond the scope of the current work, should be carried out.